Improving the specific Capacity of Nickel Hydroxide Nanocrystals for Hybrid Supercapacitors via Yttrium Doping

Yuanyi Zhu, ShengliAn, Jinlong Cui, Hengrui Qiu, Xuejiao Sun, Yongqiang Zhang*,Wenxiu He*

School of Chemistry and Chemical Engineering, Inner Mongolia University of Science & Technology, Baotou, China

*Corresponding Author：

E-mail addresses: wenxiu_he@foxmail.com (W. He), Tel.: ++86-472-5953323(W. He);

yongqiang_zhang1203@foxmail.com (Y. Zhang).

1. Experimental

1.1 Fabrication of Y-doped $Ni(OH)_2$ composites

In a typical synthesis, $Ni(NO_3)_2 \cdot 6H_2O$ (2 mmol) and $Y(NO_3)_3 \cdot 6H_2O$ (Ni/Y mole ratio of 10:1) was dissolved into 40 mL distilled water. 10 mL of 0.2 M ammonia were slowly dropped into the above solution with stirring for 30 min, and the green solution was sealed in 60 mL Teflon-lined autoclave. Then, the autoclave was heated to 180 ^oC in oven for 18 h. After cooled naturally to room temperature, the Y-Ni10 samples were collected after washed several times and dried at 80 ^oC overnight. For comparison, the Y-Ni0, Y-Ni5 and Y-Ni20 samples were also fabricated by the similar process (Ni/Y molar ratios of 0, 20:1 and 5:1).

1.2 Sample characterization

The as-prepared samples were characterized by scanning field-emission electron microscopy (SEM, Carl sigma 500 AMCS), transmission electron microscopy (TEM, Talos FEI), X-ray diffraction (XRD, Bruker, D8 ADVANCE) with Cu Kαradiation (λ = 0.15418 nm), X-ray photoelectron spectroscopy (XPS, Thermo ESCALAB 250ZI), and the nitrogen adsorption apparatus (ASAP2460, SN:543).

1.3 Electrochemical evaluation

The working electrodes were fabricated by loading the homogeneous slurry onto nickel foam. The slurry were prepared from 80% active materials, 15% acetylene black, 5% polytetrafluoroethylene and appropriate amount of ethanol solvent. The mass loading of the active material on these electrodes is around 2.1 mg/cm^2. The electrochemical properties containing galvanostatic charge discharge (GCD), cyclic voltammetry (CV) and electrochemical impedance spectroscopy (EIS) of working electrodes were tested in three-electrode glass cell with 6 M KOH electrolytes, Hg/HgO and platinum-plate were served as the reference and counter electrodes, respectively.

The Y-Ni10//AC cell was constructed by using the Y-Ni10 as the positive and active carbon (AC) as negative electrodes. The mass ratio of was obtained from the equation of $C_-\times m_-\times V_-=C_+\times m_+\times V_+$, where C_+ and C_- are the specific capacitance of Y-Ni10 and AC electrodes, V_+ and V_- are the voltage range of Y-Ni10 and AC, m_+ and m_- are the active mass loadings of Y-Ni10 and AC, respectively. According to the GCD studies of the individual Y-Ni10 and AC electrodes, the calculated mass ratio of 1:3.86 is used to balance the charges.

The specific capacitance (C, F g^{-1}), specific energy density (SE, W h kg^{-1}) and power density (SP, W kg^{-1}) of Y-Ni10//AC cell was obtained based on the following equation:

$$C = \frac{2I\int Vdt}{MV^2 \mid_{Vi}^{Vf}} \quad (1)$$

$$SE = \frac{I\int Vdt}{M} \quad (2)$$

$$SP = \frac{E}{\Delta t} \quad (3)$$

Where I (A) is the discharge current, M (g) is the total mass of Y-Ni10 and AC materials and Δt (s) is corresponding to discharge time, V_i and V_f are the cell voltage of an initial and final value,

respectively.

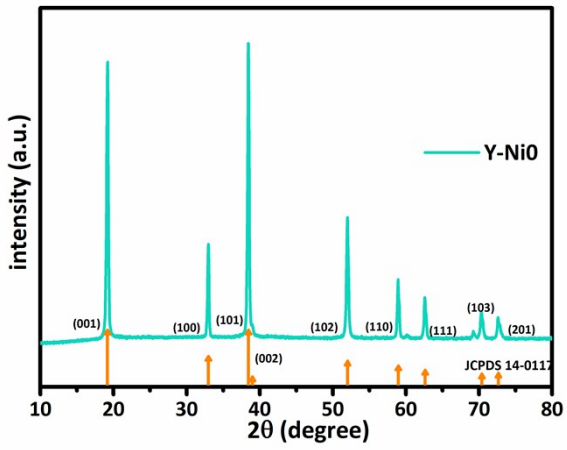

Fig. S1. XRD patterns of Y-Ni0

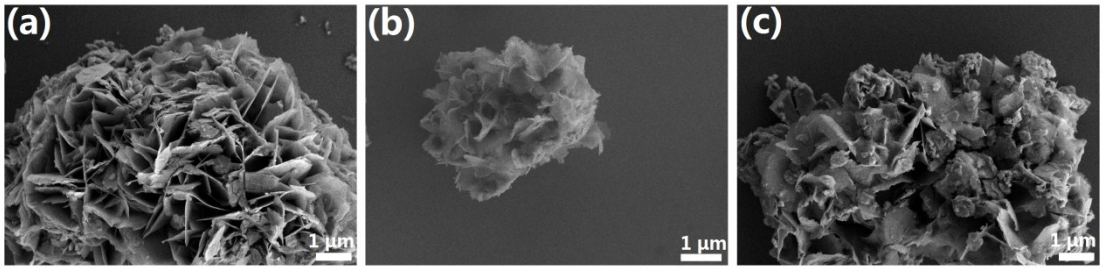

Fig. S2. SEM images of (a) Y-Ni5, (b) Y-Ni10 and (c) Y-Ni20.

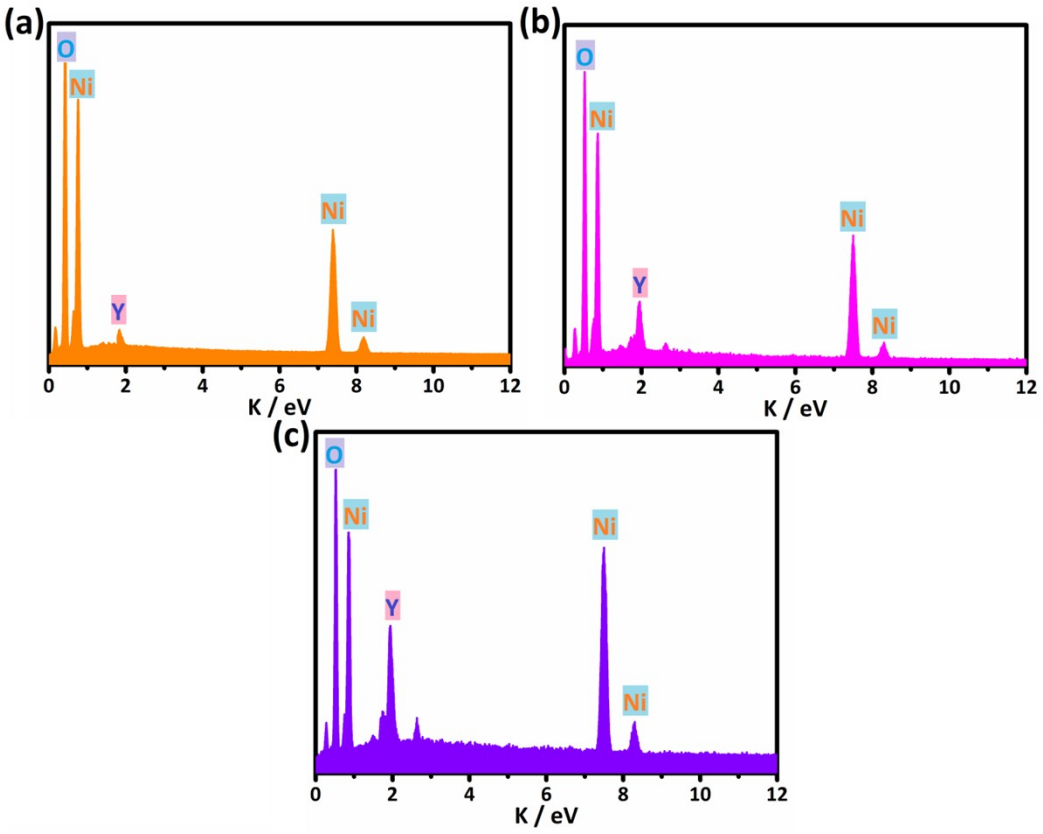

Fig. S3. EDX of the Y-Ni0, (b)Y-Ni5, (c)Y-Ni10 and (d) Y-Ni20 samples.

Table S1. the mass ratios of the Ni and Y elements in Y-Ni5, Y-Ni10 and Y-Ni20 samples.

samples	Ni norm. (wt%)	Y norm. (wt%)	Y/Ni molar ratios
Y-Ni5	52.66	3.24	4.42%
Y-Ni10	49.97	7.65	10.99%
Y-Ni20	54.45	13.98	18.43%

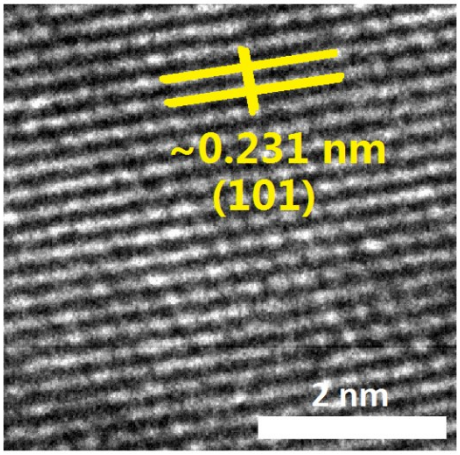

Fig. S4. HRTEM images of Y-Ni0 sample.

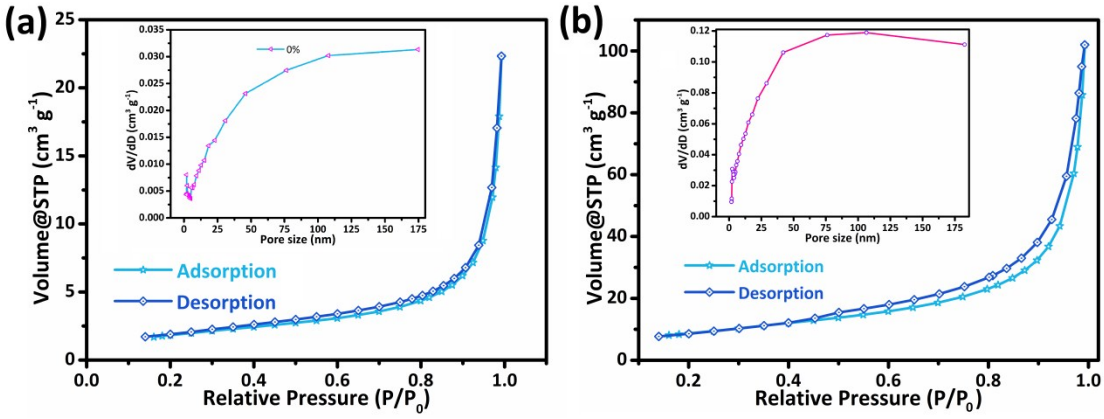

Fig. S5. N_2 absorption-desorption isotherm of (a) Y-Ni0 and (b) Y-Ni5 samples (insets of the pore distribution).

Table S2. A comparison study of BET and pore diameter.

Sample	Specific surface area	Total pore volume	Average pore diameter
	($m^2\ g^{-1}$)	($cm^3\ g^{-1}$)	(nm)
Y-Ni0	6.7931	0.034545	20.4408
Y-Ni5	32.0665	0.157677	18.3113
Y-Ni10	119.3531	0.266668	7.9563
Y-Ni20	105.2588	0.214238	7.3784

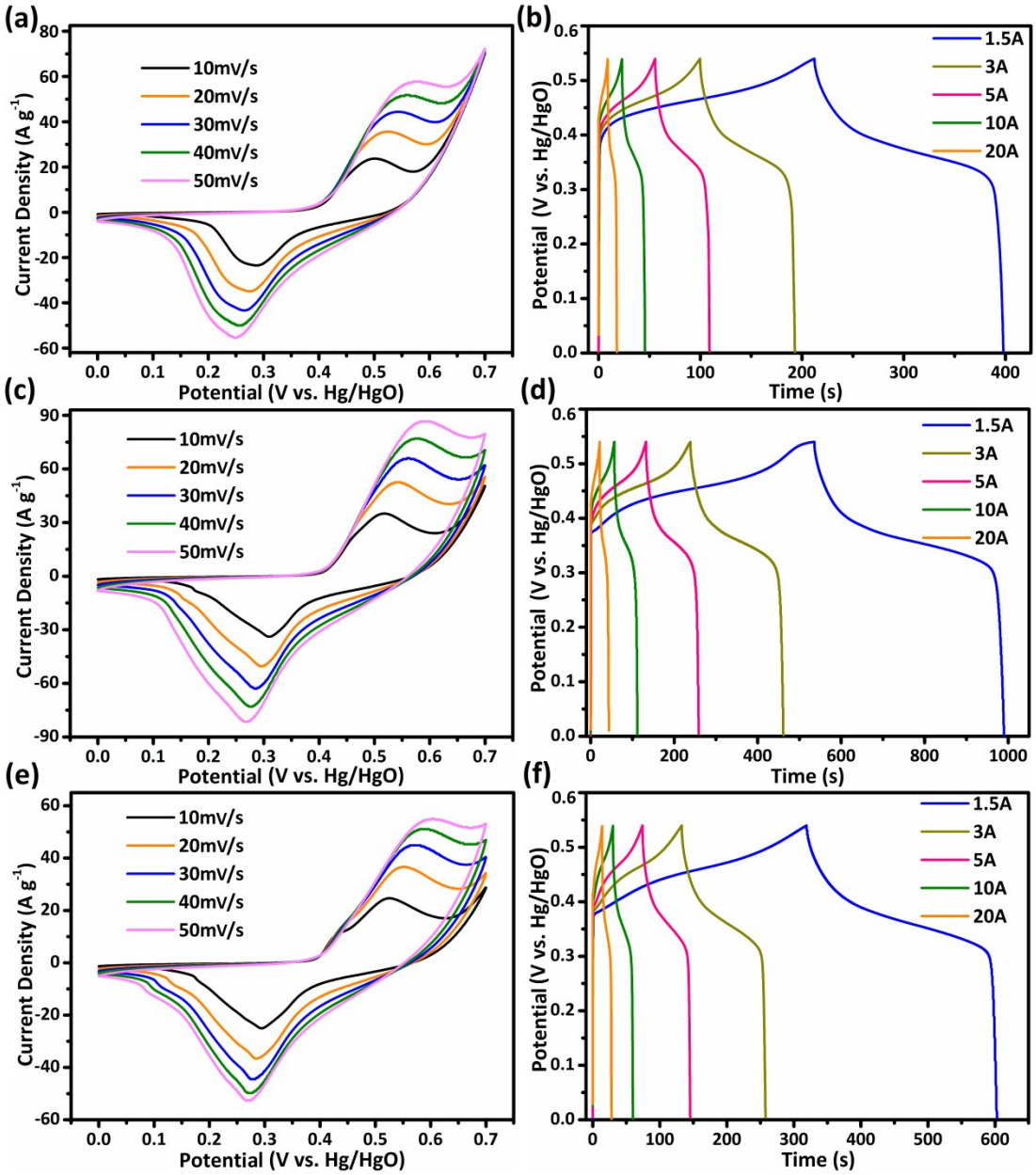

Fig. S6. CV curves at different scan rates of (a) Y-Ni0, (c) Y-Ni5 and (e) Y-Ni20, Galvanostatic charge-discharge curves of (b) Y-Ni0, (d) Y-Ni5 and (f) Y-Ni20.

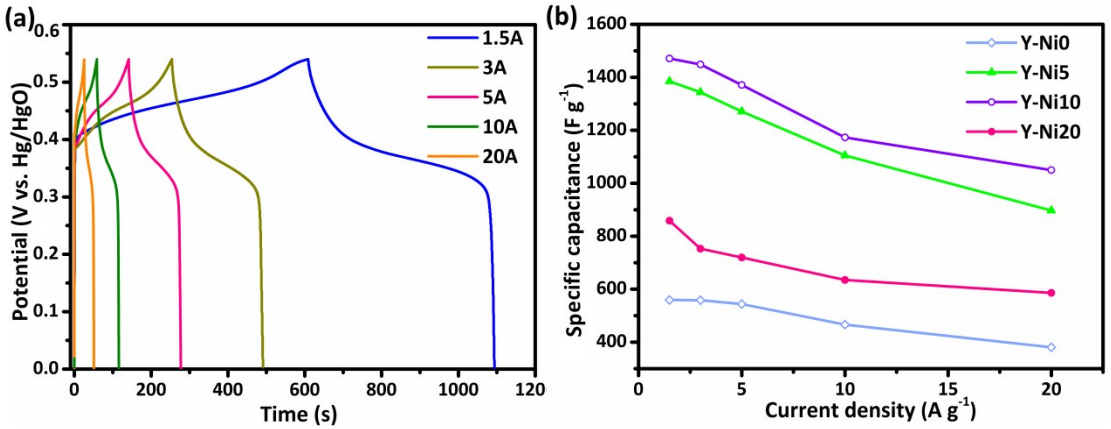

Fig. S7. (a) Galvanostatic charge-discharge curves of Y-Ni10； (b) Specific capacitance of Y-Ni0, Y-Ni5, Y-Ni10 and Y-Ni20 electrodes

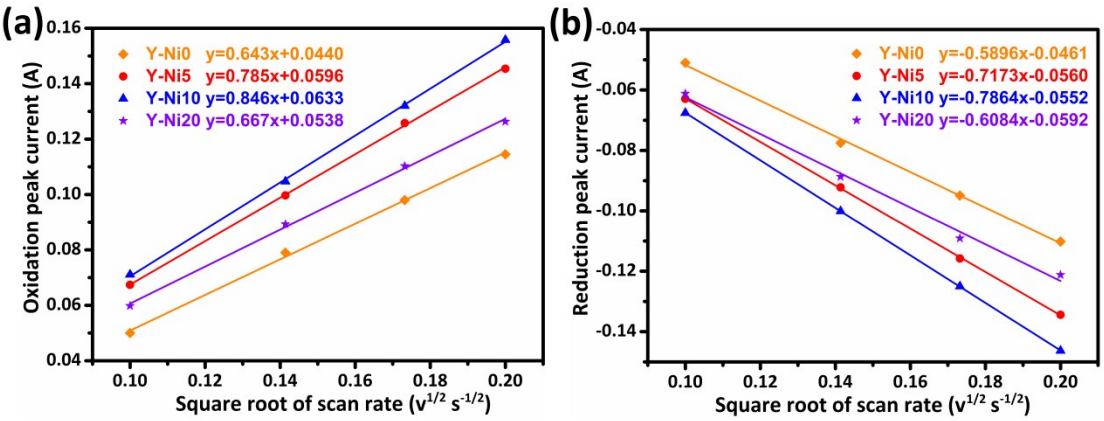

Fig. S8. the linear relation between the oxidation/reduction peak current and the scan rates of Y-Ni0, Y-Ni5, Y-Ni10 and Y-Ni20.

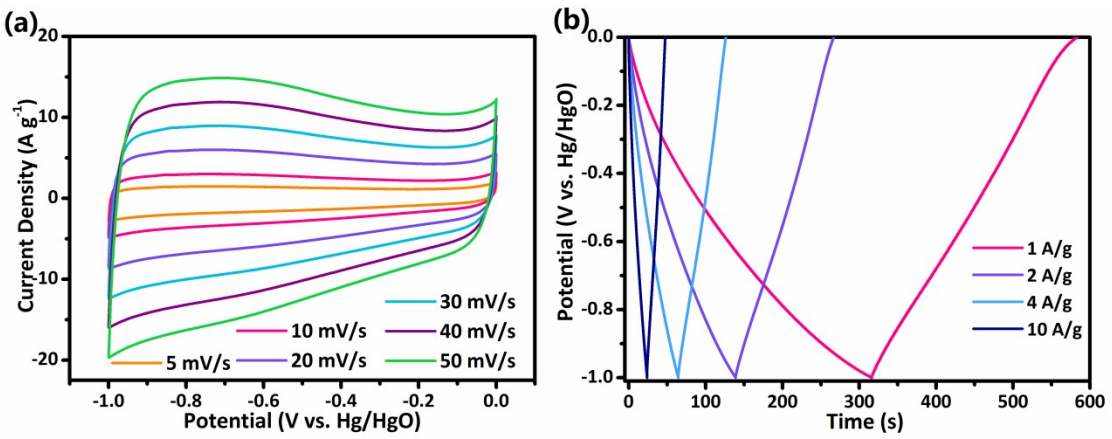

Fig. S9. CV curves at different scan rates and Galvanostatic charge-discharge curves of AC.

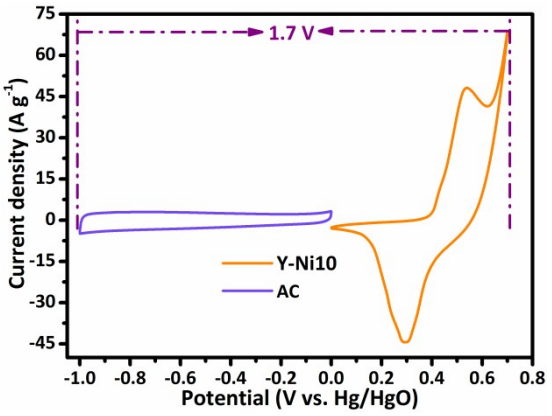

Fig. S10. (a) CV curves of the Y-Ni10 and AC electrodes in the three-electrode system at 10 mV^{-1}.

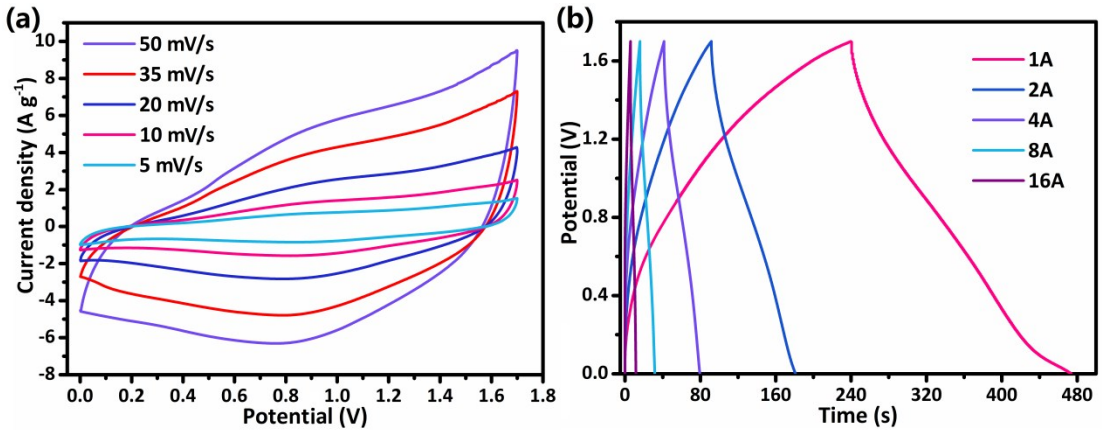

Fig. S11. (a) CV curves at different scan rates and (b) GCD curves of the Y-Ni10//AC device.

Table S2. The specific capacitance of various electrodes in the three-electrode system in references

Electrode materials	Specific Capacity	capacity retention	Refs
Ni-CO-Mn-OH/RGO	665 C g^{-1} at 2 A g^{-1}	64.21% at 20 A g^{-1}	S1
NiCoMn-OH	757 C g^{-1}at 1 A g^{-1}	48.7% at 50 A g^{-1}	S2
NiCoAl-LDH nanoplates	564.5 C g^{-1} at 1 A g^{-1}	59% at 30 A g^{-1}	S3
Co_3O_4@NiCoAl- LDH	441.6 C g^{-1} at 1 A g^{-1}	60.05% at 20 Ag^{-1}	S4
Al -$Ni(OH)_2$ nanosheets	849 C g^{-1} at 1 A g^{-1}	65.4 % at 6 Ag^{-1}	S5
CoMn LDH	531.3 C g^{-1}at 0.7 A g^{-1}	69.1% at 28.6 Ag^{-1}	S6
NiMn-LDH/rGO	625 C g^{-1} at 1 A g^{-1}	36.0% at 5 A g^{-1}	S7
Glucose NiMn-LDH	732 C g^{-1} at 1 A g^{-1}	59.4% at 10 A g^{-1}	S8
Core–Shell NiAl−LDH	367.5 C g^{-1} at 2 A g^{-1}	75.0% at 25 A g^{-1}	S9
CoAl-LDH	339.3 C g^{-1} at 1 A g^{-1}	73.6 at 20 A g^{-1}	S10
CoAl-LDH/FGN	611 C g^{-1} at 1 A g^{-1}	75.3% at 10 A g^{-1}	S11

References

[S1] B. Zhao, L. Zhang, Q. Zhang, D. Chen, Y. Cheng, X. Deng, Y. Chen, R. Murphy, X. Xiong, B.Song, C.P. Wong, M.S. Wang, M. Liu, Rational Design of Nickel Hydroxide-Based Nanocrystals on Graphene for Ultrafast Energy Storage, Adv. Energy Mater. 8 (2017) 1702247.

[S2] Y. Zhu, C. Huang, C. Li, M. Fan, K. Shu, H.C. Chen, Strong synergetic electrochemistry between

transition metals of α phase Ni-Co-Mn hydroxide contributed superior performance for hybrid Supercapacitors, J. Power Sources 412 (2019) 559-567.

[S3] J. Yang, C. Yu, X. Fan, J. Qiu, 3D Architecture Materials Made of NiCoAl-LDH Nanoplates Coupled with NiCo-Carbonate Hydroxide Nanowires Grown on Flexible Graphite Paper for Asymmetric Supercapacitors, Adv. Energy Mater. 4 (2015) 400761.

[S4] X. Li, Z. Yang, W. Qi, Y. Li, Y. Wu, S. Zhou, S. Huang, J. Wei, H. Li, P. Yao, Binder-free Co_3O_4@NiCoAl-layered double hydroxide core-shell hybrid architectural nanowire arrays with enhanced electrochemical performance, Appl. Surf. Sci. 363 (2016) 381-388.

[A5] J. Huang, T. Lei, X. Wei, X. Liu, T. Liu, D. Cao, J. Yin, G. Wang, Effect of Al-doped β-$Ni(OH)_2$, nanosheets on electrochemical behaviors for high performance supercapacitor application, J. Power Sources 232 (2013) 370-375.

[S6] A.D. Jagadale, G. Guan, X. Li, X. Du, X. Ma, X. Hao, A. Abudula, Ultrathin nanoflakes of cobalt manganese layered double hydroxide with high reversibility for asymmetric supercapacitor, J. Power Sources 306 (2016) 526-534.

[S7] M. Padmini, S.K. Kiran, N. Lakshminarasimhan, M. Sathish, P. Elumalai, High-performance Solid-state Hybrid Energy-storage Device Consisting of Reduced Graphene-Oxide Anchored with NiMn-Layered Double Hydroxide Electrochim. Acta 236 (2017) 359-370.

[S8] L. Lv, K. Xua, C. Wang, H. Wan, Y. Ruan, J. Liu, R. Zou, L. Miao, K.K. Ostrikov, Y. Lan, J. Jiang, Intercalation of Glucose in NiMn-Layered Double Hydroxide Nanosheets: an Effective Path Way towards Battery-type Electrodes with Enhanced Performance, Electrochim. Acta 216 (2016) 35-43.

[S9] M. Shao, F. Ning, Y. Zhao, J. Zhao, M. Wei, G.G. Evans, X. Duan, Core–Shell Layered Double Hydroxide Microspheres with Tunable Interior Architecture for Supercapacitors, Chem. Mater. 24 (2012) 1192-1197

[S10] S. Li, P. Cheng, J. Luo, D. Zhou, W. Xu, J. Li, R. Li, D. Yuan, High-performance flexible asymmetric supercapacitor based on CoAl-LDH and rGO electrodes, Nano-Micro Lett. 9 (2017) 31.

[S11] W. Peng, H. Li, S. Song, Synthesis of Fluorinated Graphene/CoAl-Layered Double Hydroxide Composites as Electrode Materials for Supercapacitors, *ACS Appl. Mater. Interfaces* 9 (2017) 5204-5212